Eur. Phys. J. B **11**, 121–126 (1999)

THE EUROPEAN PHYSICAL JOURNAL B

EDP Sciences

Experimental investigations of a new TGB_C mesophase

A.C. Ribeiro[1], Ph. Barois[2], Y. Galerne[3], L. Oswald[3], and D. Guillon[3,a]

[1] Centro de Fisica da Matéria Condensada (U.L.), Av. Prof. Gama Pinto 2, 1699 Lisboa Codex, Portugal
[2] Centre de Recherche Paul Pascal, CNRS, avenue A. Schweitzer, 33600 Pessac, France
[3] Institut de Physique et Chimie des Matériaux de Strasbourg, Groupe des Matériaux Organiques, 23 rue du Loess, 67037 Strasbourg Cedex, France

Received 25 January 1999

Abstract. We report on optical and structural X-ray studies on a smectic C twist grain boundary phase (TGB_C) of a pure liquid crystalline material. It is shown that this TGB_C phase, which exists over a large range of temperature, is definitely different from previously reported and predicted TGB_C phases. The two main experimental features are: (i) the observation in planar geometry of an optical texture exhibiting a square grid pattern, and (ii) the detection of a broad Bragg ring in reciprocal space instead of one (TGB_A) or two (TGB_C) sharp rings. We suggest a few possible tracks that can be explored to understand the complex structure of this new phase.

PACS. 61.30.-v Liquid crystals – 61.30.Eb Experimental determinations of smectic, nematic, cholesteric, and other structures – 61.30.Jf Defects in liquid crystals

1 Introduction

The analogy between the N-S_A phase transition and the transition from normal conductors to superconductors was established by de Gennes [1]. The possible existence of a liquid crystalline phase similar to the Abrikosov phase in type II superconductors led Renn and Lubensky to predict [2] the existence of a new frustrated smectic A phase, the "twist grain boundary smectic A" or TGB_A phase, to be observed with chiral molecules of liquid crystals, between the N^* and S_A phases. The model of molecular organization for this frustrated phase was also presented in reference [2]. In this frustrated smectic A phase where the distance between the layers is d, there are blocks of smectic A layers arranged in an helical way along an axis parallel to the smectic blocks. Two adjacent smectic A blocks are rotated by an angle $\Delta\theta$ and they are separated by a grain boundary where exists a lattice of parallel and equidistant screw dislocation lines separated by a distance l_d. The distance between two adjacent grain boundaries is l_b. The angle between two families of adjacent screw dislocation lines belonging to adjacent grain boundaries is $\Delta\theta = 2\sin^{-1}(d/2l_\text{d})$. The experimental evidence of such a phase was reported for the first time by Goodby *et al.* [3], but it is interesting to notice that all the details of a TGB_A mesophase were experimentally observed and confirmed three years later by Ihn *et al.* [4] using freeze fracture electron micrographs.

Meanwhile Lubensky and Renn [5] presented a new paper concerning the TGB phases near the N-S_A-S_C point in liquid crystals of chiral molecules. In this paper is also discussed the occurrence of the TGB_A mesophases in compounds which do not exhibit the N^* mesophase [3]. In addition, the possible existence of TGB_C and TGB_{C^*} mesophases was also predicted by Lubensky-Renn [6], and Renn [7] and the experimental evidence of the TGB_C mesophases has been demonstrated by the Bordeaux group [8] in a series of new compounds. However, the structure of the Bordeaux-TGB_C phase was found to differ from the picture originally proposed by Renn and Lubensky. In this phase, the smectic layers are tilted with respect to the helical TGB axis by an angle approximately equal to the tilt angle of molecules within each layer [9]. Finally, although no TGB_{C^*} phase has been found so far that matches the exact structure described theoretically by Renn [7], the Bangalore group [10] has reported on the experimental observation in a binary mixture of the related so-called undulated TGB_{C^*} (U-TGB_{C^*}). In this case, the model proposed involves smectic C^* blocks with a helical arrangement along the layer normal. The specific feature of the phase is the presence of undulations of the grain boundaries resulting into the formation of a square lattice in planes normal to the TGB helix [10].

In this paper, we report optical and structural X-ray studies on a TGB_C phase of a pure compound existing in a large domain of temperature. It is shown that this TGB_C phase is definitely different from the TGB_C discovered and characterized by the Bordeaux group [8]. Our experimental data are also inconsistent with other existing models (*i.e.* Renn model for TGB_C and TGB_{C^*} [6,7] and Bangalore model for U-$\text{TGB}_{\text{C}*}$ [10]). We

---

[a] e-mail: `guillon@michelangelo.u-strasbg.fr`

suggest a few tracks that should be considered for future work.

Before we proceed any further, let us notice that the number of $\mathrm{TGB_C}$ structures is increasing so much that the label $\mathrm{TGB_C}$ may be rather confusing. For the sake of clarity of the present paper, we propose to introduce a temporary classification to specify to which $\mathrm{TGB_C}$ structure we refer in particular:

R-$\mathrm{TGB_C}$: Renn-Lubensky $\mathrm{TGB_C}$ model [6];

R-$\mathrm{TGB_{C^*}}$: Renn $\mathrm{TGB_{C^*}}$ model [7];

B-$\mathrm{TGB_C}$: discovered and characterized by the Bordeaux group [8];

U-$\mathrm{TGB_{C^*}}$: discovered and discussed by the Bangalore group [10];

S-$\mathrm{TGB_C}$: present work (Strasbourg group).

2 Optical and X-ray diffraction investigations

2.1 General observations

The experimental studies reported in this paper have been performed on a compound belonging to the homologous series of sulfinate derivatives, which have been shown to exhibit $\mathrm{TGB_A}$ and $\mathrm{TGB_C}$ mesophases in large temperature domains [11]. The molecule used in the present study has exactly the same tolane core, the same linear aliphatic chain on one side, but a different branched aliphatic chain connected to the sulphur chiral part on the other. The chiral carbon centre is in the S configuration and both diastereomers with the chiral sulphur centre in the R and S configurations have been separated.

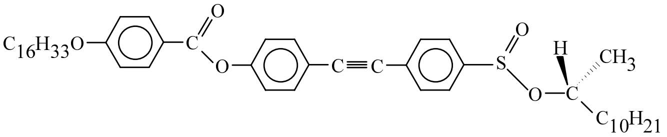

One of the diastereomers exhibits a $\mathrm{TGB_A}$ mesophase in a wide temperature range, while the other one exhibits apparently both $\mathrm{TGB_A}$ and S-$\mathrm{TGB_C}$ phases in a similar temperature domain. In this paper, we only present the results concerning the diastereomer with the two TGB mesophases.

In a first series of experiments, the characterization of mesophases along with detailed optical investigations have been performed using classical techniques, *i.e.* polarized optical microscopy, differential scanning calorimetry and X-ray diffraction on powder samples. The optical observations were made under polarizing microscope with temperature controlled Mettler and Instec hot stages. The differential scanning calorimetry measurements were performed using a Perkin-Elmer DSC7 apparatus. Powder X-ray diffraction patterns were recorded as a function of temperature using a Debye-Scherrer type camera with bent quartz monochromator ($\mathrm{K}_{\alpha 1}$ radiation, $\lambda = 1.54$ Å), an Instec hot-stage (±0.01 °C) and an INEL curved position-sensitive gas detector associated with a data acquisition computer system. The samples were housed in sealed Lindemann glass capillaries. The patterns were obtained on decreasing the temperature from the isotropic phase and registered at least during 30 minutes for each temperature.

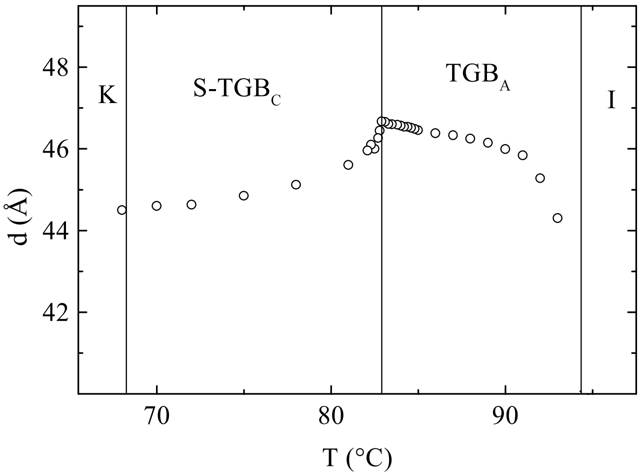

Fig. 1. Layer spacing as a function of temperature.

Two mesophases were detected by DSC and optical microscopy. Using the latter technique in the transmission mode and between crossed nicols, it was possible to observe the coexistence of cylindrical domains with planar cholesteric textures as found previously for other compounds exhibiting $\mathrm{TGB_A}$ and $\mathrm{TGB_C}$ mesophases [11]. The powder X-ray diffraction patterns registered as a function of temperature in both mesophases are typical of disordered smectic mesophases. The increase with temperature of the layer spacing in the mesophase observed at low temperature and its slight decrease with temperature in the mesophase at higher temperature are the signatures of smectic C and A phases respectively (Fig. 1). On the basis of these first observations, we cannot differentiate the present S-$\mathrm{TGB_C}$ phase from the usual B-$\mathrm{TGB_C}$. It can then be stated that the compound under consideration has the following thermal behavior:

$$\mathrm{K} \xrightarrow[59.92\ \mathrm{J/g}]{68.25\ ^\circ\mathrm{C}} \text{S-TGB}_\mathrm{C} \xleftrightarrow{82.9\ ^\circ\mathrm{C}} \mathrm{TGB_A} \xrightarrow[6.14\ \mathrm{J/g}]{94.34\ ^\circ\ \mathrm{C}} \mathrm{I}.$$

The S-$\mathrm{TGB_C}$ to $\mathrm{TGB_A}$ phase transition is observed to be second order within the accuracy of our DSC measurements.

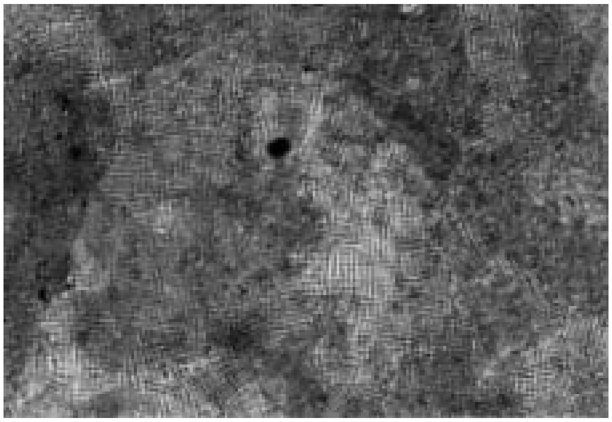

Fig. 2. Planar cholesteric texture showing the square grid in the S-$\mathrm{TGB_C}$ mesophase.

2.2 Complementary observations under optical microscope

Using a very thin preparation of the compound between two glass plates (without surface treatment and without spacers) and on cooling very slowly from the isotropic phase, the cylindrical (or marginally cone-like) domains textures in the $\mathrm{TGB_A}$ phase and in the S-$\mathrm{TGB_C}$ mesophase at lower temperature were preserved till recrystallisation [11]. The cylindrical domain texture could easily be destroyed by applying a small shear on the preparation. Then, a blue homogeneous cholesteric texture began to appear just below the transition to the isotropic phase. On decreasing further the temperature within the $\mathrm{TGB_A}$ phase, the textures remained practically the same, but all the colors of the visible spectrum were detected, from the blue one at high temperature to the red one when approaching the transition temperature between the two mesophases. The helical pitch was therefore in the range of visible light. On crossing the transition, the sample became suddenly dark and transmitted again light below 82.4 °C. The color of the texture was now grey-blue and did not change any more till recrystallisation.

In addition, a square grid rather similar to the one already observed in reference [9], was clearly visible within the described grey-blue texture as shown in Figure 2. This grid was observable from $T = 80$ °C till recrystallisation. It is also important to point out, here, that on increasing temperature from $T = 80$ °C to the transition temperature between the two mesophases the square grid was always present but collapsed at $T = 83$ °C (the $\mathrm{TGB_A}$ to S-$\mathrm{TGB_C}$ transition temperature). Finally, let us remark that the characteristic dimensions between contiguous lines in the grid did not change with temperature. Moreover, complementary optical observations in cells of different thickness (6 and 23 μm), treated to induce planar orientations, have shown that the dimensions of the square grid did not depend on the thickness of the preparation. From all these observations, the period of the grid, a, was estimated to be 1.75 ± 0.25 μm. In conclusion, this grid seemed to be intrinsic to a supramolecular organization associated with the nature of the mesophase and was the signature of a structure existing in planes perpendicular to the helical axis of the S-$\mathrm{TGB_C}$ phase.

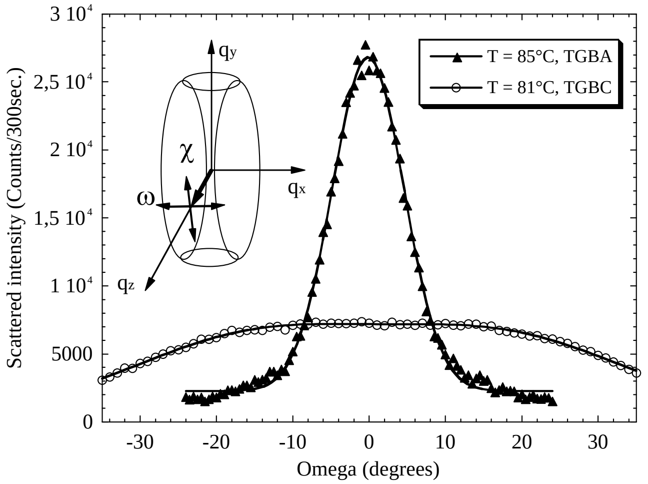

Fig. 3. X-ray scattering ω scans at constant wavevector transfer $q = 0.13$ Å^{-1}. Inset shows the scattering geometry. q_x is along the helical axis, $\omega = 0$ in the plane (q_y, q_z). Triangles are data points at 85 °C in the $\mathrm{TGB_A}$ phase. The solid line is a fit to a Gaussian function of characteristic width $\sigma = 6.6$ degrees centered at $\omega = 0$. Open circles are data points at 81 °C in the S-$\mathrm{TGB_C}$ phase.

2.3 X-ray scattering on oriented samples

In a second series of experiments, X-ray investigations on well aligned samples were performed. The samples were prepared as discussed in reference [8] between thin (50 μm) flat pieces of polymer coated and unidirectionnally buffed glass. The thickness of the liquid crystal film was fixed by two calibrated spacers, constituted by 25 μm parallel gold wires. The quality of the alignment, with the helical axis $\mathbf{x}$ perpendicular to the cell walls was checked optically under polarizing microscope. The cells were then introduced in a two stage oven (±10 mK accuracy) mounted on the X-ray spectrometer. Experiments were performed using Cu-Kα radiation of an 18 kW rotating anode X-ray generator. The samples were mounted on a 4-circles goniometer. The scattered intensity was analyzed by vertical slits and collected by a scintillator.

The scattering vector $\mathbf{q}$ is defined by the axes q_x, q_y and q_z (inset of Fig. 3). ω and χ are the rocking angles about the vertical (q_y) and horizontal (q_x) axes respectively. The X-ray optics of the spectrometer was optimized to probe the angular distribution of the layer normal (ω scans) at constant momentum transfert. The size of the X-ray beam at sample position was set to 1×3 mm^2. The in-plane resolution was then broad enough (1.2×10^{-2} Å^{-1} FWHM) to avoid two-theta (*i.e.* counter position) corrections with temperature whereas broad vertical aperture delivered the highest possible flux in order to reduce exposure times and hence sample degradation. The angular vertical resolution $\Delta\chi$ was then quite poor (of order 20 degrees FWHM) preventing any search of commensurate lockin.

Experiments were performed upon slow cooling from the isotropic phase. A series of theta-two theta scans was first performed to determine the momentum transfer $\mathbf{q}$ which was then set to an average and constant value of 0.13 Å^{-1}. ω scans recorded in the TGB$_{\rm A}$ phase exhibited the usual bell-shaped profile (triangles in Fig. 3). They are centered at $\omega = 0$, indicating that the layers are parallel to the screw axis. The ω scans are well fitted to a Gaussian profile $\exp(-\omega^2/\sigma^2)$ of characteristic width σ of order 6.6 degrees, weakly increasing upon cooling. In reciprocal vector units, it corresponds to a Gaussian characteristic width 0.015 Å^{-1} along q_x, consistent with the theoretical value $2\pi/(P_{\rm C2}d)^{1/2} \sim 0.017$ Å^{-1} expected from the RL model [2], where $P_{\rm C2}$ is the value of the helical pitch at the upper critical field, *i.e.* at the N*-TGB$_{\rm A}$ transition. It is extrapolated to about 0.3 μm in this sample. The slab thickness, $l_{\rm b}$, is then of order 150 Å with the usual assumption $l_{\rm b} \sim l_{\rm d}$ [2].

The ω scans undergo a sudden change at the TGB$_{\rm A}$ to S-TGB$_{\rm C}$ transition. The intensity profiles are much broader whereas the maximum intensity is decreased by a factor of about 4. This behaviour is clearly different from that previously reported for the B-TGB$_{\rm C}$ structure [9] in which the layer distribution function splits up into two sharp maxima. One may first suspect a sudden random disorientation of the sample at the TGB$_{\rm A}$ to S-TGB$_{\rm C}$ transition. Optical checks were performed under a microscope before and after the X-ray work on the liquid crystal cells and rule out this possibility: the optical textures appear quite regular in both phases as depicted above. An unfortunate consequence of the broadening of the ω intensity profiles is that the whole function $I(\omega)$ could not be recorded in our experimental geometry for which the limits were -35 degrees $< \omega < +35$ degrees. One may worry about the existence of intense undetected Bragg peaks at larger values of $|\omega|$. We ruled out this possibility by estimating the integral over ω of the scattered intensity, with the assumption that the observed profile is a Gaussian function (or just part of it in the S-TGB$_{\rm C}$ phase) centered at $\omega = 0$. The integral exhibits no discontinuity at the TGB$_{\rm A}$ to S-TGB$_{\rm C}$ transition and variations with temperature are consistent with similar measurements on powder samples. We conclude that the reciprocal space of the present S-TGB$_{\rm C}$ phase is well depicted by the broad bell-shaped profile also shown in Figure 3.

In addition, an important question is whether the ω profiles correspond to a broad zero-centered Gaussian function (R-TGB$_{\rm C}$ with non tilted layers [6]) or to two broad overlapping peaks at $+\omega_{\rm L}$ and $-\omega_{\rm L}$ (usual B-TGB$_{\rm C}$ with tilted layers). In the first case, the single Gaussian characteristic width σ_ω should be of order 24 degrees at 82.5 °C to 35 degrees at 81 °C. A pair of Gaussian functions centered at positions $+\omega_{\rm L}$ and $-\omega_{\rm L}$ gives slightly better fits with $\omega_{\rm L} \sim 16$ to 18 degrees and σ_ω about 23 degrees (see Fig. 4), but with one more adjustable parameter, which precludes a clear-cut conclusion. In an attempt to make a decision, we repeated the same ω scans with a transverse electric field as was done on B-TGB$_{\rm C}$ phases [12]. We observed likewise the growth of one peak only (say $\omega_{\rm L} > 0$) at constant position $\omega_{\rm L}$ (Fig. 5). We conclude that the reciprocal space is then made of two broad overlapping rings centered at positions $+\omega_{\rm L}$ and $-\omega_{\rm L}$.

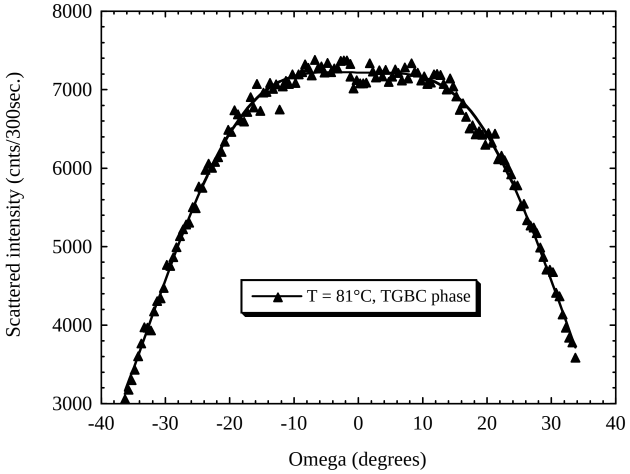

Fig. 4. Three parameters least-squares fit of the addition of two Gaussian functions onto the S-TGB$_{\rm C}$ X-ray recording of Figure 3. The tilt angle of the molecules inside the smectic layers is found to be $\theta_0 = 17°$, and the width of the Gaussian form factor of a smectic block part, $\sigma = 24°$.

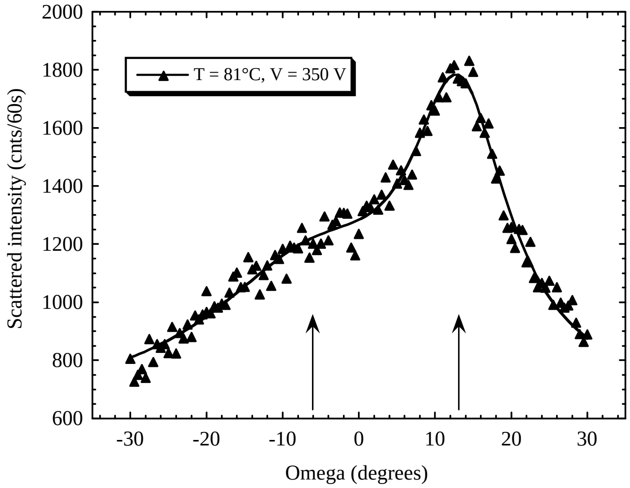

Fig. 5. Typical ω scan of a S-TGB$_{\rm C}$ sample under external transverse electric field ($T = 81$ °C, $E \sim 350$ V/3 mm). The solid line is a fit to a pair of Lorentzian functions centered at positions (denoted by arrows) $\omega_{\rm L} \sim 13$ degrees and $\omega_{\rm L} \sim -6$ degrees. The profile strongly suggests the existence of a pair of Bragg rings, distorted by the external field according to the direction of the local electric polarizations (regions with local polarization parallel to the field expand at the expense of regions with polarization antiparallel to the field) [12].

3 Discussion

X-ray diffraction patterns and optical properties described above show that the liquid crystalline phases investigated here are twist grain boundary smectic phases. Nevertheless, the present low temperature S-TGB$_{\rm C}$ is notably different from the usual B-$\mathrm{TGB_C}$ phase described by the Bordeaux group [9]; optical textures, reciprocal space and temperature range are clearly different in this sulfinate series. On the other hand, the structural models of Renn for the R-$\mathrm{TGB_C}$ and R-$\mathrm{TGB_{C^*}}$ phases seem inappropriate. Indeed, if analyzed within the frame of the RL theory, the broad width of the Bragg ring would correspond to a size of the smectic slabs l_b of order 30 $\sim$ 40 Å (depending on temperature) *i.e.* 6 to 8 molecules. Such a dramatic decrease of the slab thickness upon cooling across the $\mathrm{TGB_A}$ to S-$\mathrm{TGB_C}$ transition seems unrealistic. Furthermore, the square grid texture is clearly inconsistent with the R-$\mathrm{TGB_C}$ model (which should exhibit conventional uniform planar texture). Now, in order to explain our experimental observations, let us analyze them in the view of different possible interpretations:

(i) The first one follows the interpretation given by the Bangalore group [10]. It is essentially based upon a double helix R-$\mathrm{TGB_{C^*}}$ structure with smectic layers parallel to the TGB screw axis with the presence of undulations of the grain boundaries resulting into the formation of a square lattice in planes normal to the TGB helix. However, the origin of the $\pi/2$ angle between the directions of undulations is not explicited. Although it certainly explains the optical texture, this picture does not account for the broad distribution of the layer normal observed in our samples (Figs. 3 and 4).

(ii) A second possible interpretation does not require the presence of secondary helices. The square grid resembles much the undulations which appear above the threshold of the buckling instabilities in layered systems [13]. They are produced when changing the spacing available for the layers in the system by some external action such as, for instance, the dilation in the cell geometry or the decrease of the layer thickness upon varying temperature. Cholesterics and TGB phases can be viewed as layered systems (half pitches stack up periodically like smectic layers [14] along the helical axis). In the case of TGB phases, smectic slabs of thickness l_b form a second lattice of layers collinear with the first one. Indeed, cholesterics are well-known also to exhibit such a buckling instability, when the pitch is decreased by increasing abruptly the temperature in a planar geometry. The square grid pattern is then produced by a two-dimensional modulation of the direction of the helical axis. Such undulations of the helical axis would also explain the broadening of the Bragg ring in the X-ray pattern. Of course, the instability scenario must be ruled out here since the grid appears both ways on heating and cooling with a period that does not depend on sample thickness [15].

(iii) Extending the previous idea of undulations resulting from mechanical strain, the possibility for a similar square lattice of distorsion to develop at equilibrium in a TGB phase, as the result of the mismatch of two collinear lengths, has been proposed recently [16] but deserves further work.

(iv) Finally, we propose a structure based on the R-$\mathrm{TGB_{C^*}}$ model of Renn [7], with a few modifications though. The presence of a second helical axis within the smectic slabs (smectic C* precession) may explain the observed optical texture in the planar geometry. Following Renn, these secondary helical axes extend over the so-called helislabs [7] which stack up regularly along the main helical direction **x**. The texture will then appear as a square grid pattern provided the twist angle of adjacent helislabs locks on $\pi/2$. Furthermore, with the additional hypothesis of uniform anchoring conditions for the director at the grain boundaries, undulations of the smectic layer normal **N** are forced to develop in the plane (N, x) (Fig. 6). These new structural features clearly explain both the optical texture and the X-ray pattern [17]. The theoretical derivation of these new features will be developed in a forthcoming paper [18].

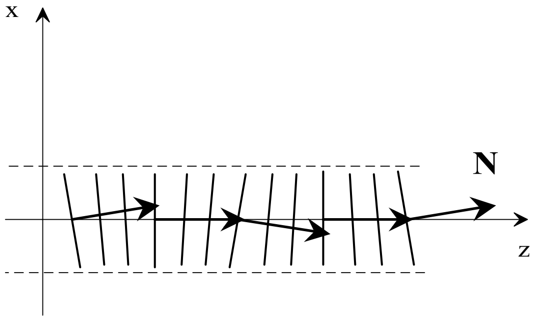

Fig. 6. Possible bend distortion of the normal to the smectic layers **N** along a smectic block, inducing compressions and dilations in the smectic layers (solid lines). **x** is the main helical axis of the TGB structure. The smectic block is limited by the classical twist grain boundaries (broken lines).

4 Conclusion

We have presented an experimental study of the TGB phases observed in a pure sulphinate compound with two chiral centres. The high temperature phase identifies well with the usual $\mathrm{TGB_A}$ phase. At lower temperature, our experiments have demonstrated the existence of a TGB phase with local smectic C order (S-$\mathrm{TGB_C}$) that clearly differs from the well characterized B-$\mathrm{TGB_C}$ phase discovered by Nguyen *et al.* [7]. The two main differences are: (i) the observation in planar geometry of an optical texture exhibiting a square grid pattern (similar to the texture reported by Pramod *et al.* [10]), (ii) the detection of a broad Bragg ring in reciprocal space instead of one sharp ($\mathrm{TGB_A}$) or two (B-$\mathrm{TGB_C}$) rings. These observations cannot be interpreted within the frame of a simple model, and consequently, the structure of this S-$\mathrm{TGB_C}$ phase seems to be complex. We do not actually propose a well established structural model for this new phase, but we suggest instead two possible tracks which can be in agreement with our experimental observations. More experimental studies are currently in progress whereas a structural model, based upon the suggested guidelines, will be proposed shortly [18].

A.C. Ribeiro wishes to thank Praxis XXI (project 3/3-1/MMA/1769/95) and University Louis Pasteur of Strasbourg for financial support, and D. Guillon for a fellowship under the same Praxis XXI project. The authors thank also the CNRS (GDR 606 “Cristaux Liquides en Géométrie Confinée”) for support in the collaboration between the different laboratories involved in this work.

References

1. P.G. de Gennes, Solid State Commun. **10**, 753 (1972).
2. S.R. Renn, T.C. Lubensky, Phys. Rev. A **38**, 2132 (1988).
3. J.W. Goodby, M.A. Waugh, S.M. Stein, E. Chin, R. Pindak, J.S. Patel, Nature (London) **337**, 449 (1989); J. Am. Chem. Soc. **111**, 8119 (1989).
4. K.J. Ihn, J.A. Zasadzinski, R. Pindak, A.J. Slaney, J. Goodby, Science **258**, 275 (1992).
5. T.C. Lubensky, S.R. Renn, Phys. Rev. A **41**, 4392 (1990).
6. S.R. Renn, T.C. Lubensky, Mol. Cryst. Liq. Cryst. **209**, 349 (1991).
7. S.R. Renn, Phys. Rev. A **45**, 953 (1992).
8. H.T. Nguyen, A. Bouchta, L. Navailles, P. Barois, N. Isaert, R.J. Twieg, A. Maaroufi, C. Destrade, J. Phys. II France **2**, 1889 (1992).
9. L. Navailles, R. Pindak, P. Barois, H.T. Nguyen, Phys. Rev. Lett. **74**, 5224 (1995).
10. P.A. Pramod, R. Pratigha, N.V. Madhusudana, Curr. Sci. **73**, 761 (1997).
11. A.C. Ribeiro, L. Oswald, J.F. Nicoud, D. Guillon, Y. Galerne, Eur. Phys. J. B **1**, 503 (1998).
12. M. Petit, P. Barois, H.T. Nguyen, Europhys. Lett. **36**, 185 (1996).
13. M. Delaye, R. Ribotta, G. Durand, Phys. Lett. A **44**, 139 (1973); N.A. Clark, R.B. Meyer, Appl. Phys. Lett. **22**, 10 (1973).
14. See for instance P.G. de Gennes, J. Prost, in *The Physics of Liquid Crystals* (Clarendon Press, Oxford, 1993), p. 293; W. Helfrich, Appl. Phys. Lett. **17**, 531 (1970).
15. In the case of buckling instabilities for lyered systems, the period of the undulations at threshold should scale as $(eD)^{1/2}$, with D the sample thickness and e the layer spacing.
16. N. Clark, *Workshop on TGB phases*, Philadelphia (April 1998).
17. A.C. Ribeiro, Y. Galerne, P. Barois, D. Guillon, L. Oswald, communication A2-03 at the 17th International Liquid Crystal Conference, Strasbourg (19-24 July 1998).
18. Y. Galerne (to be published).